

# Creep and Shrinkage of Concrete in Outdoor Exposure and Relaxation of Prestressing Steel

R. I. KINGHAM, Observer for the Canadian Good Roads Association;  
J. W. FISHER, Assistant Bridge Research Engineer; and  
I. M. VIEST, Bridge Research Engineer, AASHO Road Test, Highway Research Board

A study of the long-time behavior of prestressed concrete beams requires the determination of stress losses caused by creep and shrinkage of concrete and by relaxation of prestressing steel. Losses can be calculated accurately only if creep, shrinkage and relaxation are determined for the materials actually used in the beams. Furthermore, if the creep and shrinkage characteristics of concrete are determined by tests, the environmental conditions in such tests must approximate those to which the prestressed beams are exposed.

Outdoor creep and shrinkage tests of 24 concrete cylinders, and indoor relaxation tests of 20 samples of prestressing wire and strand are reported. The test data are described by mathematical equations obtained with the same basic model expressing shrinkage strain, creep strain or relaxation loss as a function of time. Numerical coefficients in the equations are evaluated by multiple regression analyses.

The results of the tests are used in computations of long-time strains in six prestressed concrete bridge beams. The computed strains compare favorably with the results of strain measurements on the beams.

● Studies of creep and shrinkage of concrete and relaxation of prestressing wire and strand carried out at the AASHO Road Test were made in connection with research involving four one-lane, simple-span bridges each made of three precast prestressed concrete beams and a cast-in-place reinforced concrete slab (1). Objectives of this research made it necessary to know stresses in the beams during their entire life. However, it was not convenient to make measurements except during stressing of the steel and after erection of the beams. To estimate stress changes during the intervening period, two long-term experiments were carried out on samples of materials used in the beams.

The study of shrinkage and creep characteristics of concrete was made on 24 cylinders. Two cylinders were cast in conjunction with each of the twelve bridge beams made of concrete of essentially the same quality. The experiment was conducted outdoors near the site of the prestressed concrete bridges. Observations began a few days after casting the cylinders in the fall of 1957 and continued through 1960.

The relaxation tests were made on ten samples of each type of prestressing steel. Beams for two bridges were prestressed with cables made up of parallel wires 0.192 in. in diameter; beams for the other two were prestressed with 7-wire strands of 3/8-in. diameter. The minimum length of any test was 1,000 hr. Observations of one sample of wire and two samples of strand were continued more than 9,000 hr.

The main part of this report is a general discussion of the experiments and the results of the analyses of the test data. The details of the experiments and analytical studies are contained in three appendices. The test data may be obtained in tabular form (AASHO Road Test Data Systems 2414, 2423, 2424 and 2425) from the Highway Research Board at the cost of reproduction.

## EXPERIMENTAL STUDY OF CREEP AND SHRINKAGE

The creep and shrinkage characteristics of concrete were evaluated by tests on pairs of 6- by 12-in. cylinders, as shown in Figure 1. The eight pairs in the foreground were kept under constant loads and observed for the combined effects of creep and shrinkage. The four pairs in the background were kept free and observed for the effects of shrinkage alone.

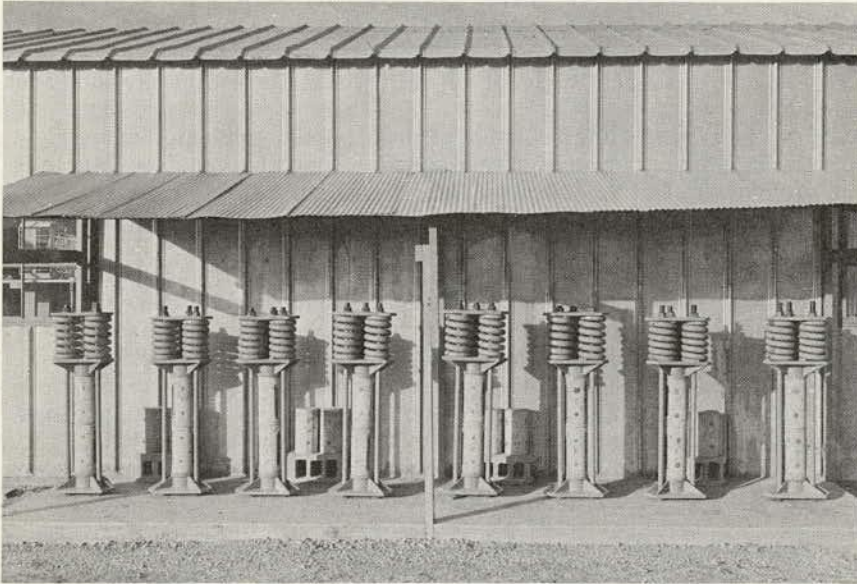


Figure 1. Creep and shrinkage tests.

The experiment included three controlled variables: the source of cylinders, the level of load, and time. An outline of the first two variables is given in Table 1.

TABLE 1  
OUTLINE OF CREEP AND SHRINKAGE EXPERIMENT

Bridge	No Load		Load = 1,000 psi			Load = 2,000 psi		
	Beam	Age* (days)	Beam	Age* (days)	Strength* (psi)	Beam	Age* (days)	Strength* (psi)
5A	3	22	2	41	7,150	1	25	6,500
5B	2	18	3	40	7,100	3	33	6,820
6A	1	13	3	13	5,850	2	21	6,330
6B	1	17	2	15	6,020	3	14	5,950

\*At beginning of test.

One pair of test cylinders was made in conjunction with each bridge beam and tested in the same loading frame. The test was designated by the combined bridge and beam designations given in Table 1; for example, the pair of cylinders made in conjunction with beam 2 of bridge 5B was observed unloaded and is referred to as test 5B2. (Because of early indications of large eccentricity of load, test 5B1 was discontinued)

after a few days and replaced by a second set of cylinders from beam 3 of bridge 5A.)

Three levels of load were chosen: 0, 1,000, and 2,000 psi. Four tests were made at each level. The load for any particular pair of cylinders is given in Table 1.

The tests were begun shortly after stressing of the corresponding beams and continued for more than three years. The strain measurements on the creep cylinders were taken immediately before and after loading and at intervals of two days to 1 1/2 months thereafter. Each time measurements were made on creep cylinders, strains were measured on shrinkage cylinders from the same bridge.

The creep and shrinkage of concrete are affected by a number of factors other than the three controlled variables of this experiment. Kept as one-level factors were the aggregates, mix proportions and water-cement ratio, curing conditions and specimen size. Other variables could be classified as uncontrolled. Of these, the most important were the age and strength of concrete at the time of loading and the environmental conditions.

These three uncontrolled variables varied with some of the controlled variables. The age and strength of concrete at the time of loading varied with the source. The changes in environmental conditions were essentially the same for all specimens, as all were tested in the same place. However, the environment changed with time.

Differences in the uncontrolled variables were determined by independent measurements. The age at loading varied from 13 to 41 days and the corresponding strength of concrete from 5,850 to 7,150 psi (Table 1). Among the environmental conditions, the temperature and relative humidity were recorded. The temperature varied between -20 F and +100 F and the relative humidity between 11 and 100 percent.

Strains were measured with a mechanical gage on three 6-in. gage lines on the surface of each cylinder. All readings were corrected for temperature effects in the concrete cylinders. The corrected readings for the six gage lines on any one pair of cylinders were generally in good agreement except for small strains. For example, for a mean strain of 0.0006 one standard deviation, based on readings on individual gage lines, was approximately 0.0001. The standard deviation increased with increasing strain but considerably less than in direct proportion.

The temperature-corrected strains for the six gage lines were averaged and the means were used in the analyses. Two typical sets of data are shown in Figure 2: one for test 6A3 representing apparent creep (i. e., the combined creep and shrinkage) in cylinders loaded to 1,000 psi and the other for test 6A1 representing shrinkage of cylinders without load. The strains are plotted against time, with unit shortenings plotted upward and unit elongations plotted downward.

The tests shown in Figure 2 were started in October 1957. The over-all trend of both the shrinkage and the apparent creep data was a shortening of cylinders with time. However, the shrinkage data showed expansion immediately after the beginning of tests and again one and two years later. A similar effect was noted on the apparent creep curve one and two years after beginning the test. On the other hand, the difference between the apparent creep and the shrinkage, labeled as corrected creep, was largely independent of this cyclic effect.

It is believed that the cyclic effect was, at least in part, the result of cyclic variations in the environmental conditions. In fall and winter the humidity was relatively high and the temperature low: the cylinders absorbed moisture and expanded. In spring and summer the humidity decreased and the temperature increased: the cylinders dried and shrank.

It was apparent from the corrected creep curves that the creep strains in loaded cylinders increased rapidly at first. By 1,100 days the creep strains were increasing at a very slow rate, giving evidence that the creep might be approaching a finite value. Shrinkage was essentially completed, except for the seasonal variations, by the end of the first year.

The corrected creep data at any particular time showed marked differences from specimen to specimen. This is illustrated in Table 2, which includes creep strains that accumulated in 1,150 days. The specimens are listed in the order of decreasing age at loading, and the strains are given per psi of load. On the average, this unit

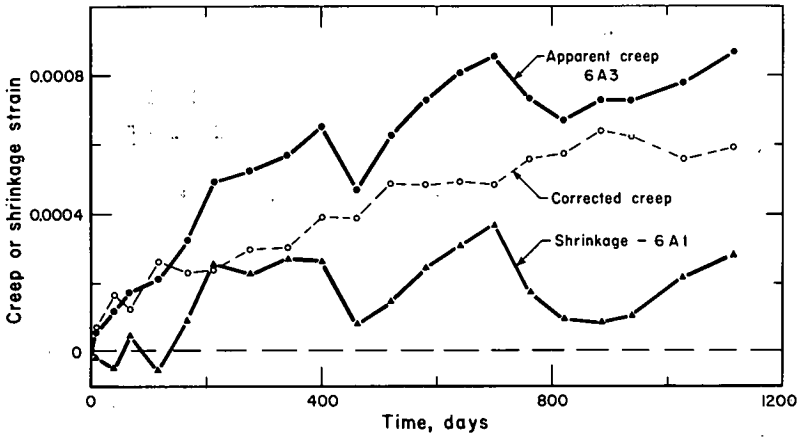


Figure 2. Typical creep and shrinkage data.

creep was about the same for the cylinders subjected to 1,000 psi and for those subjected to 2,000 psi, indicating that creep was proportional to load. A more detailed examination of the data suggested an increase in creep with decrease in the age of cylinders at loading.

TABLE 2

INSTANTANEOUS STRAINS AND CORRECTED CREEP STRAINS IN 1, 150 DAYS

Load = 1,000 Psi				Load = 2,000 Psi			
Test	Strain per Psi*		Creep Initial	Test	Strain per Psi*		Creep Initial
	Initial	Creep			Initial	Creep	
5A2	0.196	0.242	1.2	5B3	0.236	0.464	2.0
5A3	0.175	0.540	3.1	5A1	0.217	0.445	2.1
6B2	0.252	0.593	2.4	6A2	0.235	0.571	2.4
6A3	0.254	0.544	2.1	6B3	0.246	0.578	2.3
Mean	0.219	0.480	2.2	Mean	0.233	0.515	2.2

\*Strain in micro-inches per inch divided by the magnitude of load.

Table 2 also includes initial strains per unit load caused by the application of load. The unit initial strains were larger for the greater loads and for younger specimens. The ratio of creep in 1,150 days to the initial strain was of the order of 2.2. Although further testing might have shown further increases in creep strains, it was apparent that to attain significant increases the period of observation would have had to be extended considerably.

EXPERIMENTAL STUDY OF RELAXATION

The relaxation characteristics of prestressing steel were evaluated by studies of 20 60-in. specimens of wire and strand tested in steel frames, as shown in Figures 3 and 4. Each specimen was stressed to the desired level and anchored at both ends. The distance between the anchorages, approximately 40 in., was constant throughout

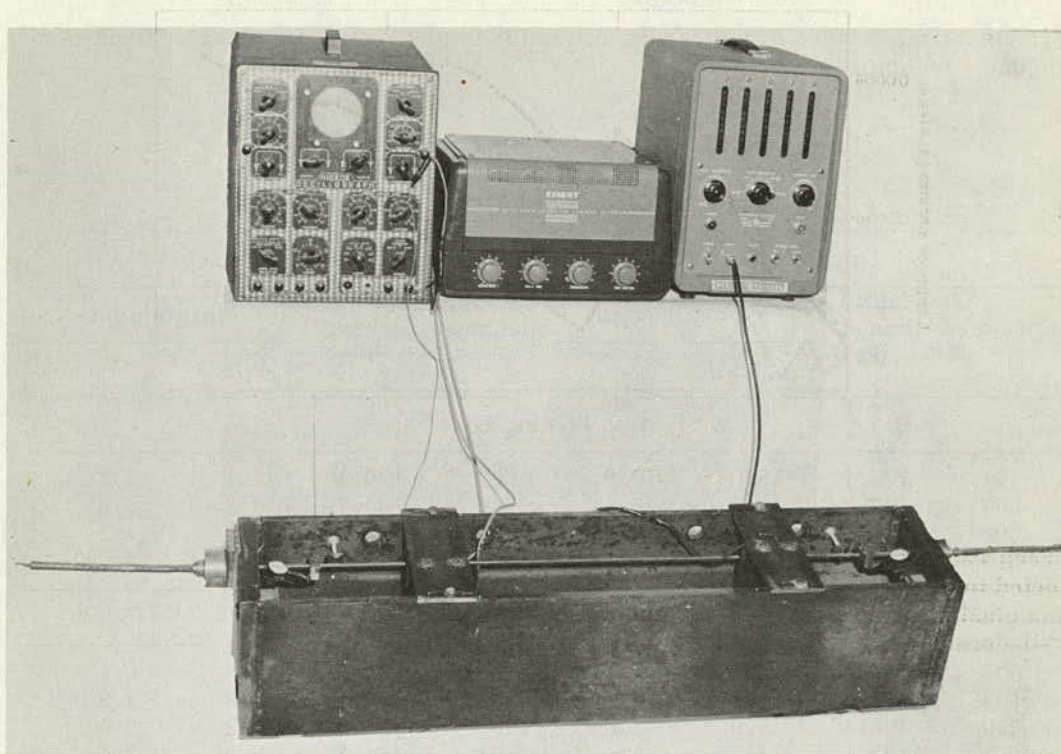


Figure 3. Relaxation test of wire.

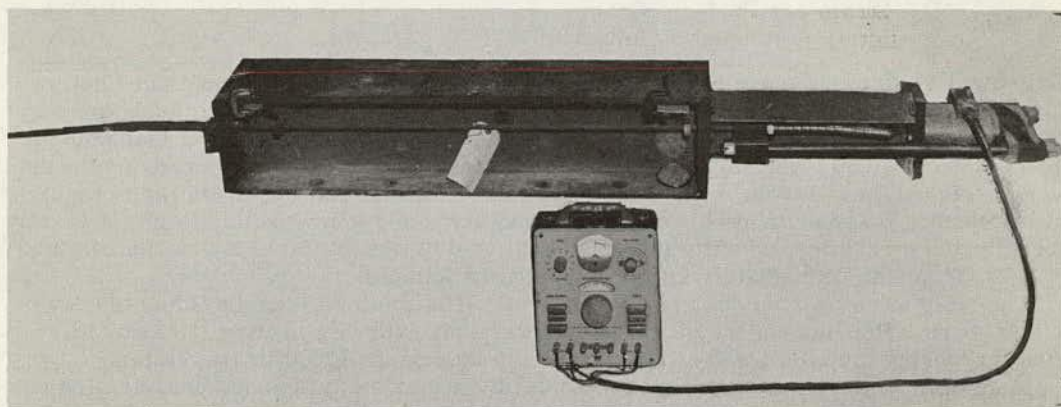


Figure 4. Relaxation test of strand.

the experiment. The changes in the stress level in the specimens were determined at intervals by measuring the changes in the fundamental frequency of the wire specimens (Fig. 3) and with the aid of a load cell in the strand specimens (Fig. 4).

The experiment included four controlled variables: the type and the source of prestressing steel, the level of initial stress, and time. The first three variables are listed in Table 3.

Two types of cold-drawn prestressing steel were used in the bridge beams: stress-relieved wire and stress-relieved strand. Each was furnished in two shipments.

From specimens taken during fabrication of the beams, five were selected from each shipment for the relaxation study.

TABLE 3  
RELAXATION LOSSES IN 1,000 HOURS

Shipment A				Shipment B			
Specimen	Initial Stress, $f_i$ , (ksi)	Relaxation loss		Specimen	Initial Stress, $f_i$ , (ksi)	Relaxation loss	
		$r$ , (ksi)	%			$r$ , (ksi)	%
(a) 0.192-In. Wire*							
509	199.1	18.0	9.0	507	196.4	14.1	7.2
506	187.5	14.8	7.9	505	184.7	10.8	5.8
502	180.8	13.0	7.2	504	180.5	7.7	4.3
510	169.1	8.1	4.8	503	175.0	7.3	4.2
(b) 3/8-In. Strand <sup>+</sup>							
604	187.5	10.2	5.4	606	195.5	11.9	6.1
609	185.0	11.9	6.4	608	189.0	8.2	4.3
610	165.4	5.0	3.0	603	185.8	7.2	3.9
607	163.0	4.2	2.6	601	169.3	5.3	3.1
602	158.0	3.1	2.0	605	168.3	5.9	3.5

\*Ultimate strength,  $f_s^u = 257$  ksi for both shipments.

<sup>+</sup>Ultimate strength,  $f_s^u = 265$  ksi for shipment A, 275 ksi for shipment B.

Only eight tests of wire are reported in this paper. One test was discontinued before 1,000 hr as a result of accidental movement of the testing frame, which made questionable a portion of the results; the other because of faulty experimental techniques.

Two stress levels were selected for both types of prestressing steel and specimens were assigned these levels at random. However, initial seating of anchorages required overstressing the specimens for a short period and made it impossible to attain exactly the selected stress levels. The initial stress levels given in Table 3 were determined by measurements immediately after anchoring the samples.

The tests were carried out in 1959 and 1960. The minimum length of any test was 1,000 hours. Readings of the stress levels were taken during loading, immediately after anchoring the steel, and at intervals from 90 sec. to 1,000 hr thereafter.

In addition to the four controlled variables, the experiment included uncontrolled variations in the quality of steel and in the environmental conditions. Control tests indicated that all steel in any one shipment had essentially the same mechanical properties and chemical composition. The variations in environmental conditions were not recorded but were believed to have been relatively small because the tests were carried out in a heated room.

Typical data from one relaxation test are shown in Figure 5. Strand specimen 609, selected for this figure, was stressed initially to 185 ksi. The relaxation loss in 1,000 hr was 11.9 ksi, or 6.4 percent of the initial stress. Observations beyond 1,000 hr showed substantial losses at later ages: e. g., at 5,000 hr the loss was 40 percent in excess of the 1,000-hr loss.

The rate of relaxation loss decreased with time. The log-log plot in the lower portion of Figure 5 illustrates that within the duration of these tests the relaxation losses followed closely a logarithmic straightline relationship. Thus the data gave no definite

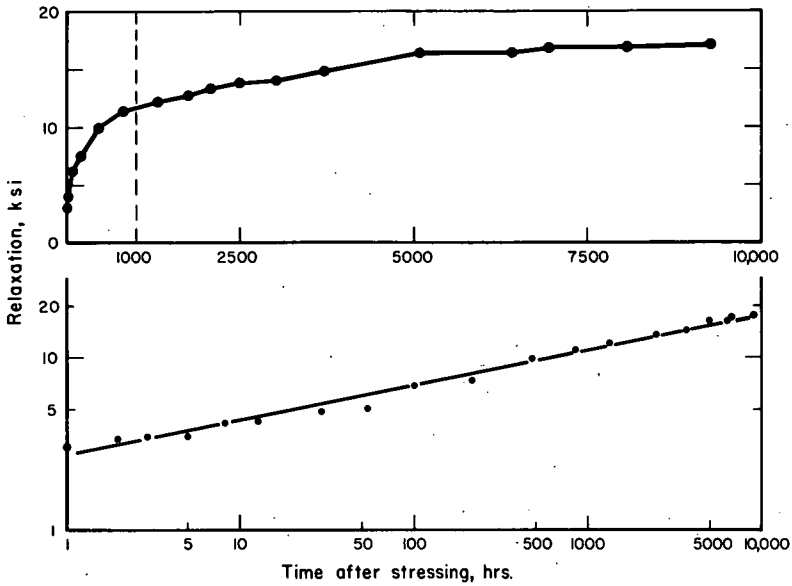


Figure 5. Typical relaxation data, specimen 609.

indication whether the relaxation loss would approach a finite limiting value at later ages.

The relaxation loss in 1,000 hr is given for all specimens in Table 3. It is apparent that the relaxation loss increased with increasing initial stress and was smaller for wire B than for wire A. The relaxation loss for strand B appeared to be somewhat lower than that for strand A.

#### ANALYSIS OF TEST DATA

The objective of this study was to develop a reliable basis for estimating the time-dependent losses in prestressed concrete beams. This objective could be met by statistical correlations of shrinkage and creep strain and relaxation stress with time. The correlations required first the selection of mathematical models suitable for regression analyses.

The primary criterion in the choice of the final model was the degree of correlation between observed test data and corresponding values calculated from the evaluated model. However, it was also considered desirable, although not essential for the objective of this study, for the model to satisfy the following three characteristics of creep, shrinkage (without the cyclic effects), and relaxation:

1. At time  $t = 0$ , the deformation (or stress loss)  $\Delta = 0$ .
2. At  $0 < t < \infty$ ,  $\Delta$  increases at a decreasing rate.
3. At  $t = \infty$ ,  $\Delta$  reaches a finite value  $\Delta_{\infty}$ .

Several models found in the literature were examined in the original as well as in various modified forms. Of these, the simple exponential model used by Shank (2)

$$\Delta = at^b \quad (1)$$

and the semilogarithmic model used by Raphael (3)

$$\Delta = a \ln(t + 1) \quad (2)$$

could be fitted satisfactorily only to limited ranges of the test data. Furthermore, they did not satisfy the third characteristic. A modification of the exponential Eq. 1, proposed by Stüssi (4), although satisfying all three characteristics, fitted satisfactorily

only the relaxation data.

Another simple model studied by several investigators (5, 6, 7) and satisfying all three desired characteristics may be written in the form

$$\Delta = \Delta_{\infty} (1 - e^{-t/a}) \tag{3}$$

which could not be fitted accurately to the full range of creep observations, indicating that the rate of creep did not follow the simple relationship on which the equation is based (that is, that the rate of creep is at all times proportional to the amount of potential creep remaining). McHenry (5) proposed a series of additive terms to correct for this discrepancy. A similar multiple-term model, proposed by Freudenthal and Roll (6), was found in excellent agreement with their test data.

Both McHenry's and Freudenthal and Roll's expressions are unsuitable for fitting through linear regression analysis. It was noted, however, that the rate of deformation increase indicated by Eq. 3 may be modified by the following adjustment:

$$\Delta = \Delta_{\infty} (1 - e^{-t/a})^b \tag{4}$$

in which

- $\Delta$  = time deformation or stress loss at time  $t$ ;
- $\Delta_{\infty}$  = total potential time deformation or stress loss;
- $t$  = time; and
- $a, b$  = empirical constants.

The general shape of Eq. 4 is shown in Figure 6. It will be noted that the model satisfies the three characteristics of time deformations. Furthermore, it may be linearized as

$$\log \Delta = \log \Delta_{\infty} + b \log (1 - e^{-t/a}) \tag{4a}$$

and is, therefore, suitable for linear regression analysis. (However, it is necessary to choose the constant  $a$  arbitrarily. Thus a series of analyses is needed to determine the best values of  $\Delta_{\infty}$ ,  $b$ , and  $a$ ).

It may be noted further that for small values of  $t/a$ , the term  $(1 - e^{-t/a})$  approaches the value of  $t/a$ . In such case Eq. 4 is reduced to a simple exponential expression of the type used by Shank (2), and may be linearized as

$$\log \Delta = \log (\Delta_{\infty}/a^b) + b \log t \tag{4b}$$

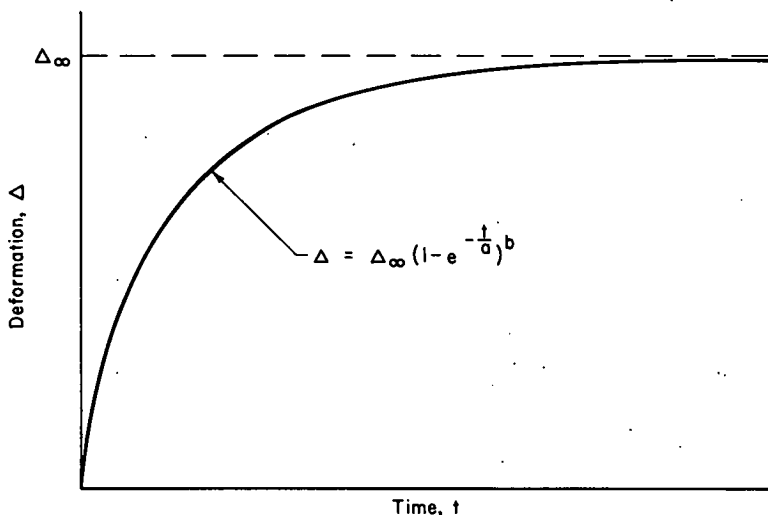


Figure 6. Time-deformation relationship.

The linearized Eq. 4a and 4b were fitted to the individual creep and relaxation tests and to the moving averages of all shrinkage data. (The moving averages rather than the original data were used in order to eliminate cyclic variations.) The ranges of the resulting coefficients of correlation (Table 4) indicate that Eq. 4 is an excellent representation of the time-deformation and time-stress loss relationships observed in this investigation.

TABLE 4  
CORRELATION FOR INDIVIDUAL SPECIMENS

Type of Test	Number of Analyses	Range of $r^{2*}$
Creep	7 <sup>+</sup>	0.86-0.98
Shrinkage	1	0.99
Wire	8	0.98-0.99
Strand	10	0.87-0.99

\* $r$  = coefficient of correlation.

+Analysis for test 5A2 not included.

The term  $\Delta_{\infty}$  in Eq. 4 represents the total potential time-deformation or time-stress loss. If it is expressed in terms of the known variables of the tests, such as the load and the properties of the material, a generalized model is established for the multiple regression analysis of all data pertaining to one problem. This procedure was used in separate analyses of the creep, shrinkage and relaxation data, as shown in the following sections.

The test observations were continued even after the completion of analytical studies. Furthermore, the data obtained during early periods of tests were subject to large percentage errors, which were magnified by the logarithmic linearization. For these reasons, only certain portions of the test periods were utilized in the analytical studies, as is indicated in the following text.

### Shrinkage Equation

The analysis of shrinkage was made in two steps: the first step determined the best fit to the test data without regard to the cyclic effects and the second step determined a correction factor, accounting for the cyclic effect. The analyses utilized only data obtained between October 28, 1957, and December 19, 1959.

After eliminating the cyclic effects by the method of moving averages, a regression analysis of the shrinkage data made on the basis of Eq. 4a resulted in the following expression for the long-time trend:

$$\Delta_s' = 0.00028 (1 - e^{-t/166})^{0.50} \quad (5a)$$

in which  $t$  is the time in days from casting the concrete.

The residuals obtained as the difference between the shrinkage data and  $\Delta_s'$  followed a cyclic trend with season. A regression analysis of the residuals based on the equation of a sine wave gave the following expression for the second term of the shrinkage equation:

$$\Delta_s'' = 0.000087 (1 - e^{-t'/10}) \sin \frac{\pi}{182} (t' + 60) \quad (5b)$$

in which  $t'$  is time in days from January 1. (For example,  $t'$  for February 15 of any year would be 45 days.)

The complete equation representing the shrinkage data of this investigation is then:

$$\Delta_s = 0.000280 (1 - e^{-t/166})^{0.50} - 0.000087 (1 - e^{-t/10}) \sin \frac{\pi}{182} (t' + 60) \quad (5)$$

in which

- $\Delta_s$  = shrinkage strain at time  $t$ ;
- $e$  = base of natural logarithm;
- $t$  = time from casting the cylinder, in days; and
- $t'$  = time from January 1, in days.

Eq. 5 is compared with the test data in Figure 7. The full lines represent the portions obtained by the analysis of the test data; the dashed lines represent extrapolations. The mean absolute residual strain for the data used in derivation of Eq. 5 is 0.000043.

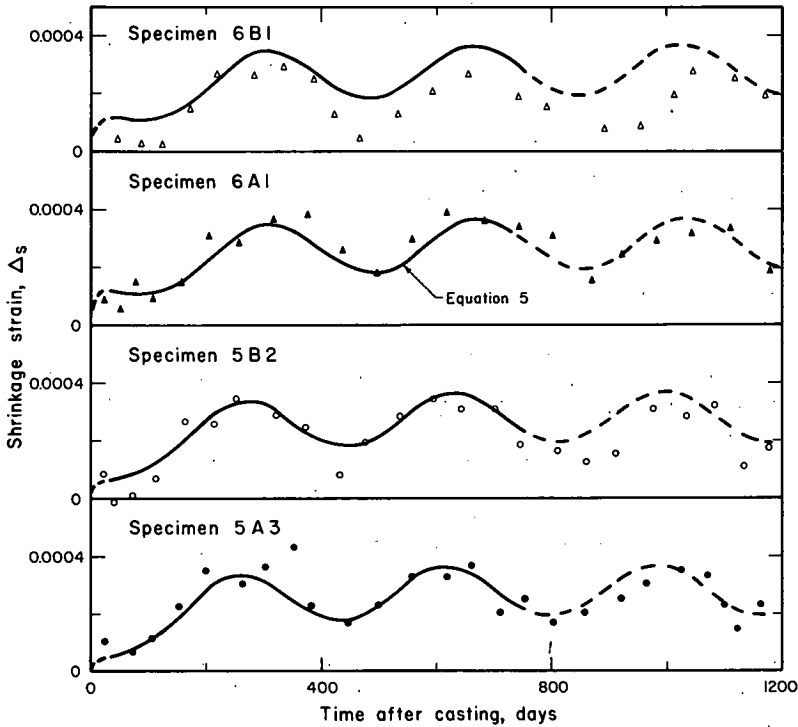


Figure 7. Correlation of shrinkage data.

### Creep Equation

Earlier studies of creep have shown that the total potential creep is a function of the magnitude of load and of the age at the time of loading (5). More recent studies have indicated that the effect of this age may be accounted for by expressing the load as a percentage of the strength of concrete at the time of loading (7). Thus, the total potential creep may be expressed as

$$\Delta_{\infty} = c(f_c/f'_{ci})^d \quad (6a)$$

in which  $c$  and  $d$  are empirical constants.

The data from six creep tests corrected for shrinkage were analyzed with multiple regression techniques on the basis of Eq. 4a combined with Eq. 6a. (Data from test 5A2 showed behavior radically different from that observed for the other specimens and were, therefore, excluded from the analysis. To avoid bias in relation to the load

level, data from test 5A1 were also omitted from the regression analysis.) Only observations made between 100 and 1,150 days after loading were included. The resulting creep equation was found to have the form:

$$\Delta_c = 0.00356 \left( \frac{f_c}{f_{ci}} \right)^{0.96} (1 - e^{-t/500})^{0.73} \quad (6)$$

in which

- $\Delta_c$  = creep strain at time  $t$ ;
- $f_c$  = load per unit area of concrete;
- $f_{ci}$  = strength of concrete at the time of loading;
- $e$  = base of natural logarithm; and
- $t$  = time from loading the concrete, in days.

Eq. 6 is compared with test data in Figure 8. It will be noted that the data for specimen 5A1, not included in the analysis, are in reasonable agreement with the theoretical line; but the data for 5A2, also excluded from the analysis, fall substantially below the regression line as well as below the range of all other test points. The mean absolute residual for the data included in the analysis is 0.000062.

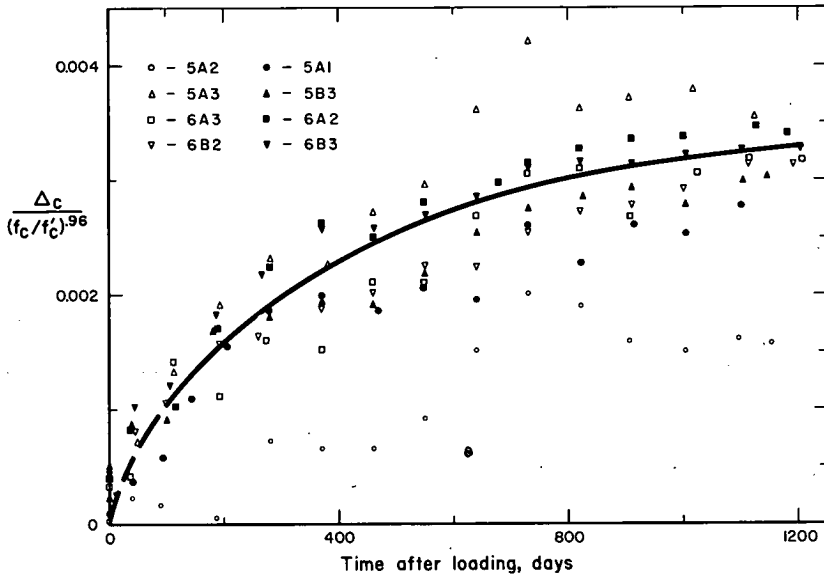


Figure 8. Correlation of creep data.

The measurements on creep cylinders determined the apparent creep, including both creep and shrinkage. This apparent creep was computed for the six tests utilized in the creep analysis as a sum of values given by Eq. 5 and 6 and is compared with the measurements in Figure 9. It will be noted that all data are located close to the line of equality. The mean absolute residual for the data shown is 0.000087.

In Figures 8 and 9, the data for specimens loaded to 1,000 psi are shown as open symbols and the data for specimens loaded to 2,000 psi are shown as full symbols. It will be noted that the equations appear to fit both sets of data equally well.

It has been pointed out in connection with the discussion of the creep experiment that the rate of increase of creep strains was very slow at 1,150 days, the terminal point of the analysis. The analytical studies indicated that equally good correlation with the test data could be obtained by the choice of several different sets of constants

greater than the set used in Eq. 6. However, constants significantly different from those used gave total potential creep substantially in excess of the creep observed at 1, 150 days.

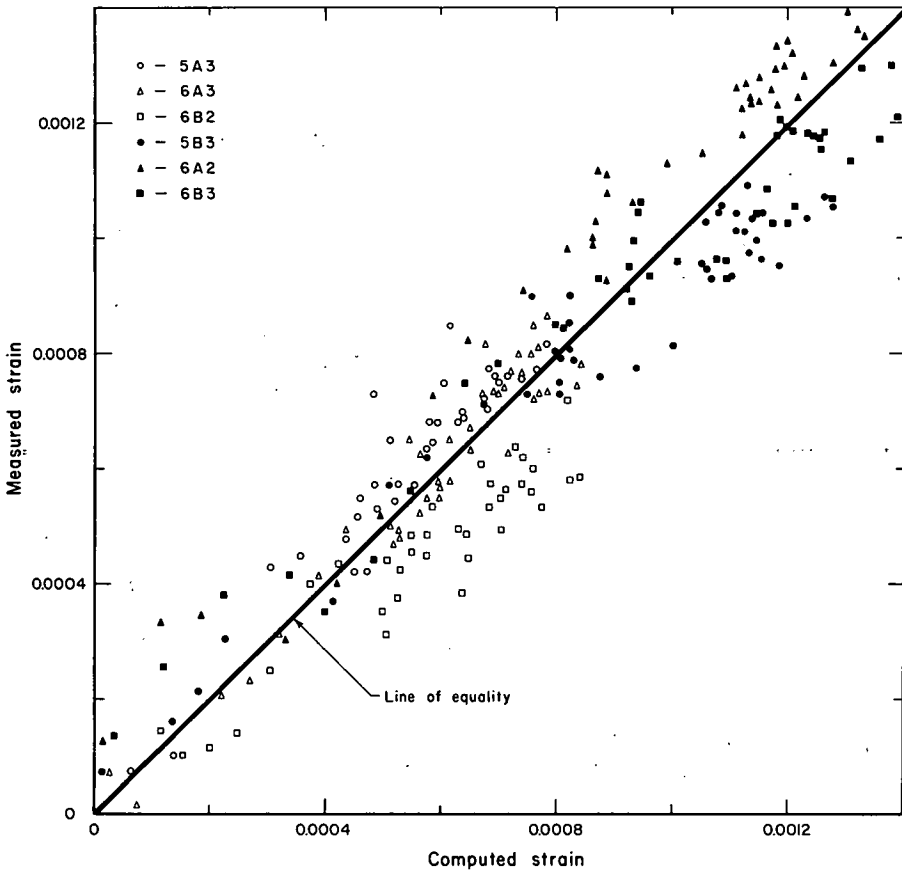


Figure 9. Comparison of computed and measured apparent creep strains.

### Relaxation Equations

The relaxation data obtained in this investigation showed a logarithmic straight-line relationship and thus gave no indication concerning the total potential relaxation loss. Furthermore, the authors were unaware of any published data indicating directly either the probable magnitude of the potential loss or the variables which have influence on it. (Stüssi's study (4) suggested that several years of observations are needed even to reach one-half of the total potential loss; i. e., the half-life. Of the experimental data utilized by Stüssi only one test appeared to approach the half-life.) However, studies of the current relaxation tests of strand have shown that the correlation between the individual specimens may be improved if the potential stress loss is expressed as

$$\Delta_{\infty} = c f_i \left( \frac{f_i}{f_s} \right)^d \quad (7a)$$

Thus, Eq. 4 may then be written in the form:

$$\Delta_r = c f_i \left( \frac{f_i}{f_s} \right)^d \left( 1 - e^{-t/a} \right)^b \quad (7b)$$

In view of the linear relationship between  $\log \Delta_r$  and  $\log t$ , the term  $(1 - e^{-t/a})$  in Eq. 7b may be replaced by the term  $t/a$ . Thus Eq. 7b may be given in the form:

$$\Delta_r = g f_i \left( \frac{f_i}{f_s} \right)^d t^b \quad (7)$$

in which

- $\Delta_r$  = relaxation stress loss at time  $t$ ;  
 $f_i$  = initial stress;  
 $f_s$  = ultimate strength of steel;  
 $t$  = time from application of initial stress, in hours; and  
 $g, d, b$  = empirical constants.

Eq. 7 does not indicate that the stress loss approaches a finite value. This is consistent with the trend shown by the test data. However, it is believed that the stress loss would have approached a finite value if the tests had been continued for a considerably longer period. In such case, Eq. 7b rather than Eq. 7 would have been better used for the regression analysis.

Using test data from 10 to 1,000 hr, the empirical constants of Eq. 7 were determined by multiple regression analysis based on Eq. 4b combined with Eq. 7a. Separate analyses were made for the strand, wire A and wire B. The results were as follows:

Type of Steel	$g$	$b$	$d$
Strand	0.0488	0.274	5.04
Wire A	0.1020	0.238	6.08
Wire B	0.0313	0.284	4.28

The correlation between Eq. 7, using these constants, and the test data is shown in Figures 10, 11, and 12. In all three figures open symbols are used for specimens subjected to lower initial stress levels. No definite bias with respect to the stress levels may be noted in any of the three figures.

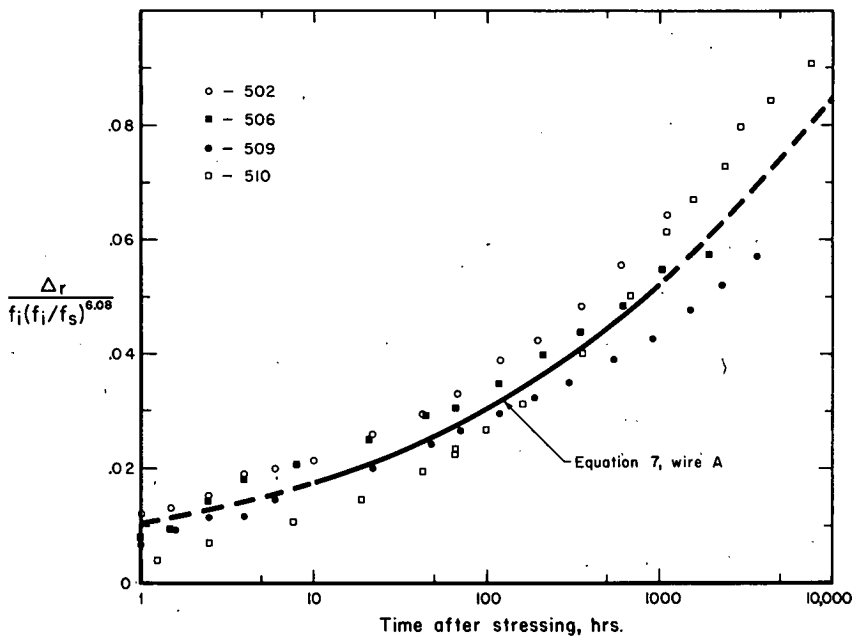


Figure 10. Correlation of relaxation data for wire A.

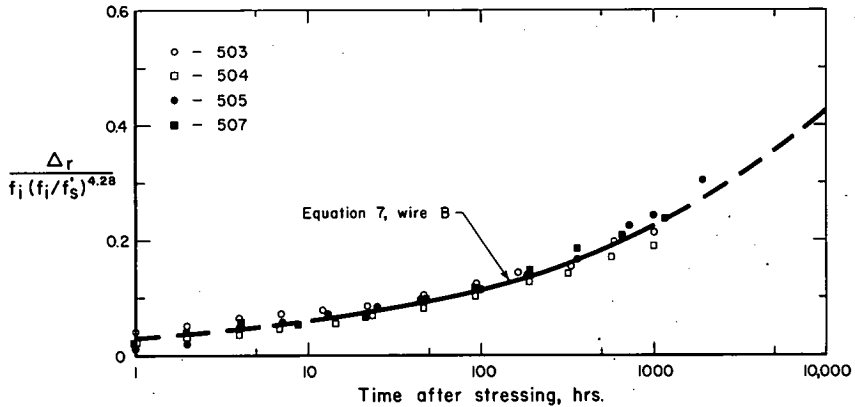


Figure 11. Correlation of relaxation data for wire B.

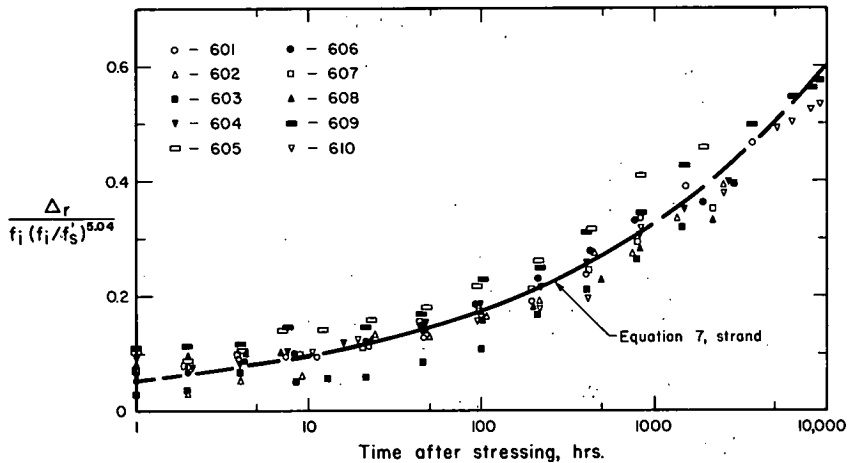


Figure 12. Correlation of relaxation data for strand.

Beyond 1,000 hr Eq. 7 is shown as a dashed line, because it represents an extrapolation. However, even the dashed lines are in reasonable agreement with the test data. The data are available up to 9,000 hr.

The mean absolute residuals for the data used in the analyses are 0.59, 1.12, and 0.38 ksi for the strand, wire A and wire B, respectively.

## COMPARISON OF RESULTS WITH OTHER MEASUREMENTS

### Relaxation Tests of Strand

The relaxation tests were made on short specimens of steel. Earlier experiments with wire indicated a good correlation between results of tests involving 100-ft specimens (8) and those involving 3-ft specimens (9). On the other hand, no data on the relaxation characteristics of strand were available. It was considered desirable, therefore, to check on the possible length effect by supplementary tests.

Two 100-ft specimens of the strand from shipment A, designated 631 and 632, were tested in the stressing bed described by Everling (8). The relaxation data for specimens 631 and 632 are plotted in Figure 13. Also included is the curve of Eq. 7 and the upper

and lower envelopes of the test data for short specimens of the strand.

The data for the 100-ft specimens follow the same general trend as Eq. 7 and fall within the range of the test data for the short specimens. It is further interesting to note by comparison with the data in Figure 12 that the results of specimens 605 and 631, having the same initial stress, showed practically identical relaxation losses; and specimens 607 and 632, also having the same initial stress, showed practically identical relaxation during the first 100 hr.

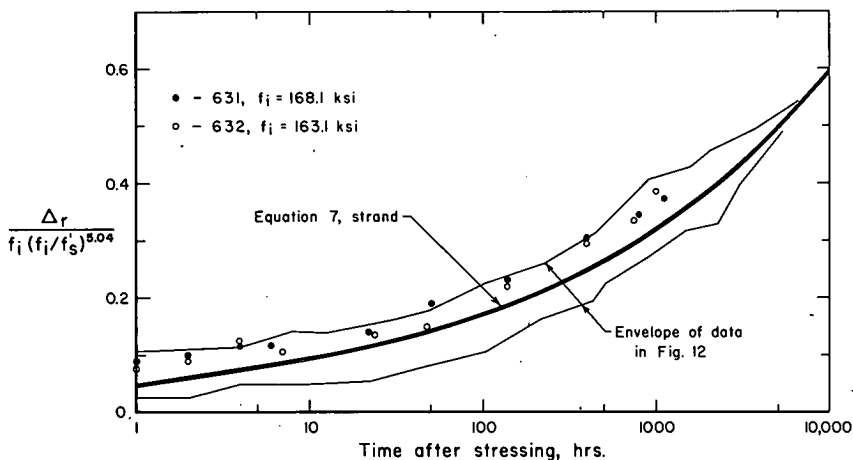


Figure 13. Relaxation tests of 100-ft strands.

### Time Losses in Prestressed Concrete Beams

The six post-tensioned beams for the test bridges at the AASHO Road Test were erected four months before casting the slab (1). The change in the bottom flange strains during this period may be computed on the basis of the shrinkage, creep and relaxation characteristics represented by Eq. 5, 6, and 7, and compared with the measured change.

In a beam, the shrinkage and creep of concrete, and the relaxation of prestressing steel, are accompanied by decreases in the prestressing force. Thus, the time deformations in a prestressed concrete beam occur under a varying stress. Of the several methods accounting for this variation in stress (10), the rate of creep method was selected for this study. (The rate of creep method was compared on one beam with the superposition method. For the interval considered in this paper, there was no significant difference between the results of the two methods.) A numerical integration procedure, described elsewhere (11), was used on the basis of twelve intervals of nine to eleven days.

The computed strains are compared with measurements in Table 5. Although the measured strains were usually lower than the computed ones, the differences for beams 5A2, 5A3, 5B1 and 5B2 were within the accuracy of the measurements. For beams 5A1 and 5B3 the measured strains were considerably below the computed quantities. It should be noted, however, that the measured strains for these two beams are inconsistent with the trends indicated by measurements on the other four beams.

### SUMMARY

1. Tests of 24 concrete cylinders and 20 samples of prestressing wire were made to determine the creep, shrinkage and relaxation characteristics for use in the interpretation of the tests of prestressed concrete bridges. The cylinders were tested for

TABLE 5  
COMPARISON OF COMPUTED AND MEASURED LOSSES IN  
PRESTRESSED CONCRETE BEAMS\*

Beam	Date of Casting	Age at Stressing (Days)	$f'_c$ (psi)	Computed Partial Strains( $\times 10^6$ )				Total Strain( $\times 10^6$ )		Measured Computed
				$\Delta c$	$\Delta s$	$\Delta r$	$\Delta el$	Computed	Measured	
5A1	509	3	4600	150	135	-61	-18	206	108	0.52
2	480	13	5850	106	113	-69	-12	138	129	0.93
3	508	5	5050	136	135	-86	-17	168	153	0.91
5B1	391	97	8100	154	72	-120	-19	87	97	1.11
2	496	4	4950	226	127	-133	-27	193	172	0.89
3	496	3	4600	257	127	-134	-30	220	94	0.43

\*Losses between the dates 5<sup>4</sup>3 and 6<sup>5</sup>4 for bridge 5A and between the dates 533 and 654 for bridge 5B. Dates relate to consecutive numbering, with 391 = July 27, 1957.

more than three years in an outdoor exposure. The samples of steel were tested for at least 1,000 hr. The results were correlated by multiple regression analyses utilizing one basic model for all three phenomena.

2. The results of shrinkage tests are represented by Eq. 5, including the effects of age and of seasonal variations. Pronounced seasonal variations, believed to be the result of environmental changes, were observed in the tests of both shrinkage and creep cylinders.

3. The results of creep tests are represented by Eq. 6, indicating the existence of a maximum potential creep. The potential creep is expressed as a function of the ratio of the applied stress and the strength of concrete at loading.

4. The results of the relaxation tests are represented by Eq. 7, having different empirical constants for the strand, wire A, and wire B. The equation should not be applied beyond 9,000 hr, representing the upper limit of the test data.

5. Satisfactory comparisons with measurements made on the companion prestressed concrete beams indicated that the equations form a suitable basis for computing the stress losses in these beams.

#### ACKNOWLEDGMENTS

The study reported herein was carried out as a part of the bridge research at the AASHTO Road Test. The authors wish to acknowledge the contributions of all those who were connected with various phases of the investigation and particularly the many helpful suggestions made by Dr. Paul Irick, Chief of Data Analysis, during the course of planning the experiment and of data analysis.

The relaxation tests of the 100-ft strands were made by the laboratories of the American Steel and Wire Division, United States Steel Corporation.

#### REFERENCES

1. Viest, I. M., "Bridge Research at the AASHTO Road Test." HRB Spec. Rep. 38, pp. 24-43 (1958).
2. Shank, J. R., "The Plastic Flow of Concrete." Ohio State Univ. Eng. Exper. Sta., Bull. 91 (1935), 62 pp.
3. Raphael, J. M., "The Development of Stresses in Shasta Dam." Am. Trans. ASCE, 118: 289-309 (1953).
4. Stüssi, F., "On Relaxation of Steel." Intern. Ass. for Bridge and Struct. Eng. Publ., 19: 273-286 (1959).
5. McHenry, D., "A New Aspect of Creep in Concrete and Its Application to Design." Proc. ASTM, 43: 1069-1084 (1943).
6. Freudenthal, A. M., and Roll, F., "Creep and Creep Recovery of Concrete under High Compressive Stress." Am. Proc. Con. Inst., 54: 1111-1142 (1958).
7. Lyse, I., "Shrinkage and Creep of Concrete." Am. Proc. Con. Inst., 56: 775-782 (1960).

8. Everling, W. O., "Discussion of Steel Wire for Prestressed Concrete." Proc., First U. S. Conf. on Prestressed Concrete, Mass. Inst. of Technology, pp. 161-166 (1951).
9. McLean, G., and Siess, C. P., "Relaxation of High-Tensile-Strength Steel Wire for Use in Prestressed Concrete." ASTM, Bull. 211, pp. 46-52 (Jan. 1956).
10. Ross, A. D., "Creep of Concrete under Variable Stress." Am. Proc. Con. Inst., 54: 739-758 (1958).
11. Corley, W. G., Sozen, M. A., and Siess, C. P., "Time-Dependent Deflections of Prestressed Concrete Beams." HRB Bull. 307 (1962).

## *Appendix A*

### DETAILS OF CREEP AND SHRINKAGE EXPERIMENT

#### Specimens

The aggregates used in the 6- by 12-in. concrete cylinders were lake sand and crushed stone. The lake sand, mostly siliceous, had an average fineness modulus of 2.67; the coarse aggregate, with a maximum size of 1 in., was a crushed limestone. Sieve analyses for sand and gravel are given in Table 6.

TABLE 6  
GRADATION OF AGGREGATES

Crushed Stone		Sand	
Sieve Size	Retained (%)	Sieve Size	Retained (%)
1 1/2	0.0	3/8	0.0
1	0.2	No. 4	3.2
3/4	19.8	No. 8	12.8
1/2	61.0	No. 16	26.1
3/8	81.9	No. 30	46.1
No. 4	97.3	No. 50	80.6
No. 8	98.0	No. 100	97.8
		No. 200	99.4

The concrete, made with type I portland cement furnished by one manufacturer, had the following characteristics: Cement content, 7.00 sacks per cubic yard; water content, 4.6 gal per sack; mix proportions by weight (cement: sand: crushed stone), 1:1.74:2.86; air-entraining agent, approximately 3/4 oz per sack; average slump, 1 5/8 in.; and air content, 3.1 to 5.0 percent.

The amount of air-entraining agent was adjusted according to the control tests of air content. Concrete was compacted with internal vibrators and steam cured for 12 to 84 hr with a maximum temperature of 110 F. Concrete cylinders were delivered to the bridge site with their respective beams and kept with the beams until the start of testing.

In addition to those reserved for the creep and shrinkage experiment, several cylinders were prepared for compression tests. Results of the compression tests are shown in Figure 14. Cylinders were tested at the time of stressing the bridge beams, at 28 days, and at the beginning of test traffic. A mean strength value was found for each of the three groups and the curve shown in Figure 14 was fitted to the three means. The strengths given in Table 1 were taken off the mean curve.

The coefficient of thermal expansion of the concrete was found to vary between 0.000048 and 0.000075 per  $^{\circ}\text{F}$  when temperature varied between 37 and 100 F.

### Testing Apparatus and Instrumentation

The loading frame for creep tests consisted of a yoke made up of steel plates, tie bars and springs shown schematically in Figure 15. Two concrete cylinders were placed end on end and separated by a steel plate. The cylinders were capped with a high-strength gypsum plaster to insure uniform distribution of load. The load was applied by tightening the nuts on the tie bars to deflect the springs, which transmitted the load to the cylinders through the loading head.

Concrete cylinders for shrinkage tests were placed on end near the creep cylinders. They, of course, required no loading frame.

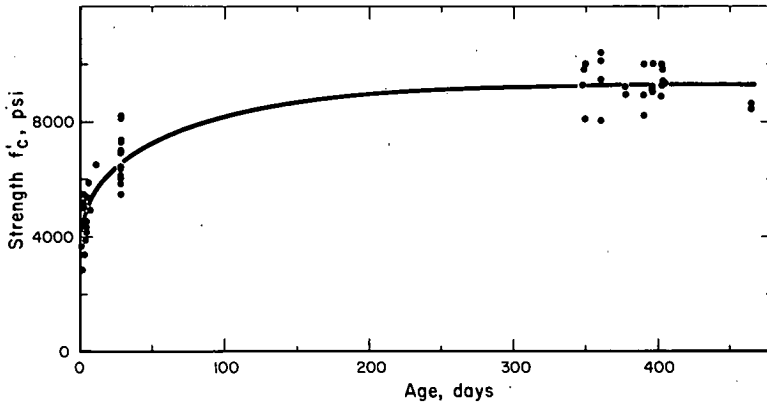


Figure 14. Cylinder strength of concrete.

The creep cylinders were instrumented for measurement of longitudinal strains on six equidistant gage lines spaced around the circumference on the surface. Electric resistance strain gages 6 in. long were placed on every other gage line. On each remaining gage line, two brass plugs spaced at 6 in. provided reference points for measurements with a mechanical gage. The plugs were fitted tightly into shallow holes drilled in the cylinders, and held by epoxy resin. The distance between two small holes in the brass plugs was measured with a Metzger gage. One division on the dial of the gage was equal to the strain of 0.000149.

The shrinkage cylinders had only the three gage lines for measurements with the mechanical strain gage.

The load was determined from the deflection of the springs. Each spring had two reference holes approximately 10 in. apart when unloaded and was calibrated with several increments of load. The rate of spring deflection was approximately 0.0001 in. per lb. The deflections were measured with a caliper graduated to 0.01 in.

### Testing Procedure

After the creep cylinders were assembled in the frame, initial readings were taken on all twelve gage lines. Then the load was applied in three increments. After each increment, the electric strain gages were read to check the concentricity of the load. Differences in the strains on the three gages served as a basis for distribution of the following load increment to the three springs. After the total load was applied and distributed to the three springs so as to result in essentially equal strain on all electric gages, another set of readings was taken on all twelve gage lines. The time required for loading one set of cylinders varied from 1 to 5 hr.

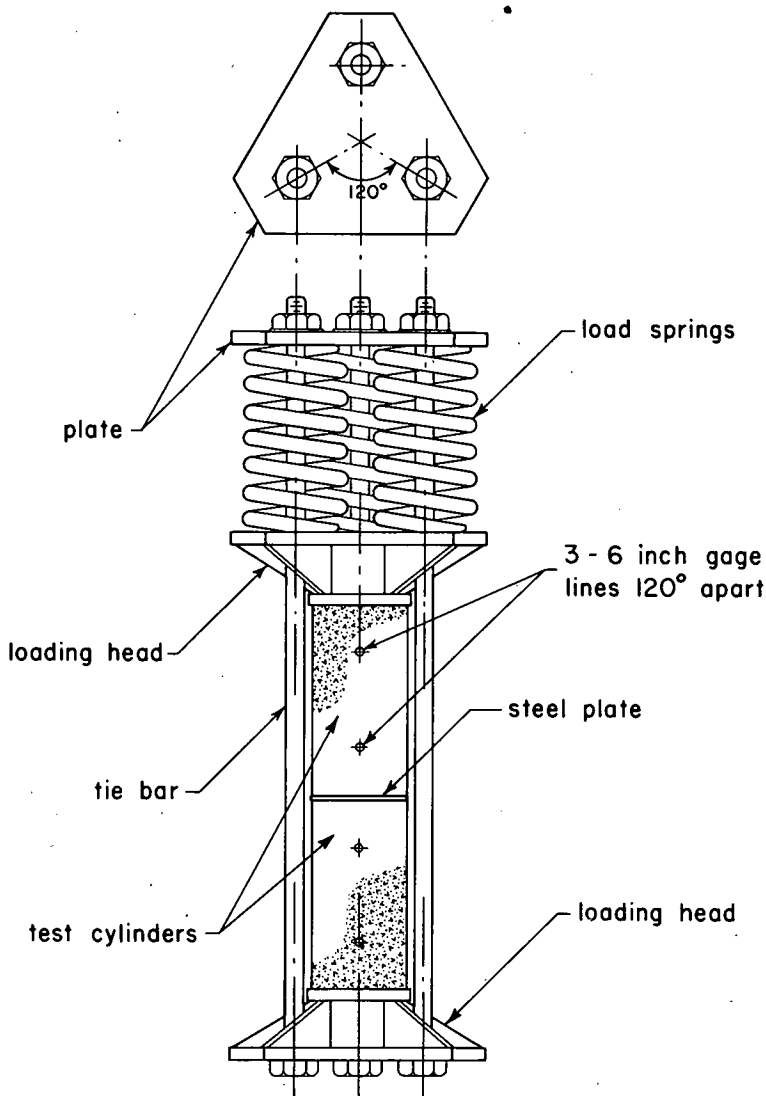


Figure 15. Loading frame for creep tests.

The mechanical strain measurements on creep cylinders were repeated every other day during the first week after loading, weekly during the following three weeks, every three weeks during the next seven months, monthly during the next two years, and every month and a half thereafter.

Each time readings were taken on a set of creep cylinders, several readings were made also on a standard bar, on shrinkage cylinders from the corresponding bridge, and on springs. Whenever the spring measurements indicated a deviation of more than 75 psi from the desired stress in the cylinders, the load was adjusted.

The air temperature was recorded near the test site every hour. The daily maxima and minima were averaged for every month (see Fig. 16).

The relative humidity data were obtained from the tables of Local Climatological Data of the U. S. Weather Bureau in Peoria, Ill. The daily maxima and minima were averaged for every month.

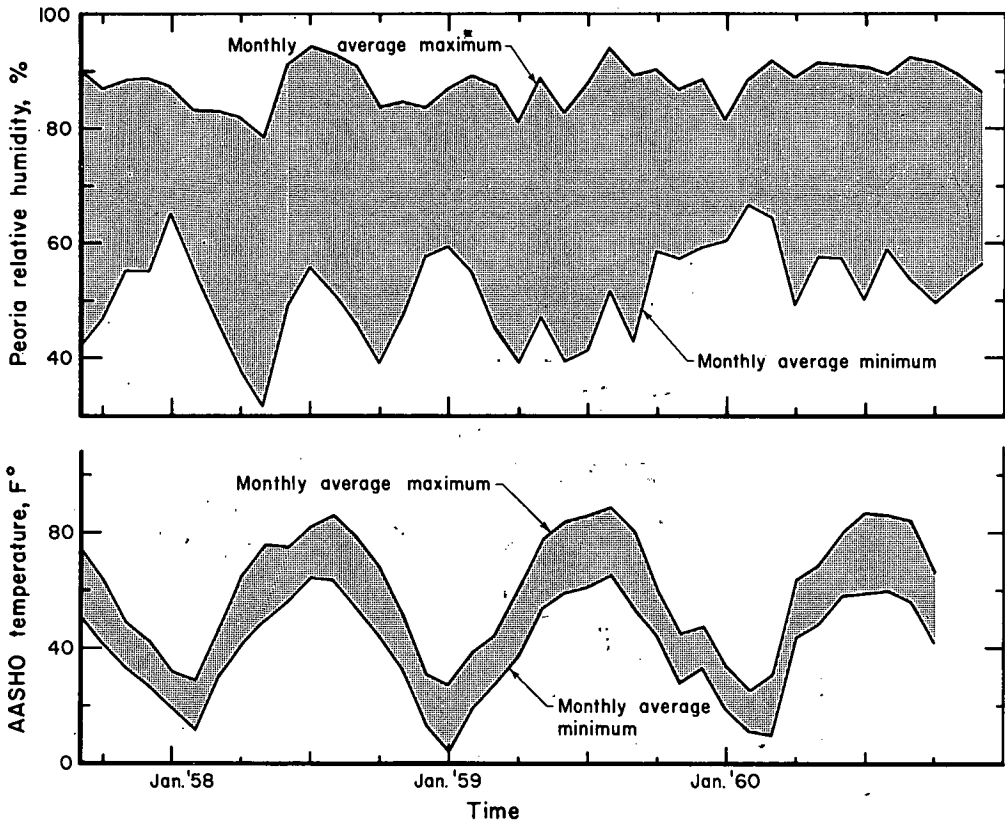


Figure 16. Relative humidity and air temperature history.

## Appendix B

### DETAILS OF RELAXATION EXPERIMENT

#### Specimens

The prestressing wire was cold-drawn and stress relieved with bright, smooth surface. The wire, produced by the John A. Roebling's Sons Corp., was delivered in approximately 55-ft lengths enclosed in flexible metal sheathing. One length of prestressing wire was taken from each shipment for relaxation tests.

The prestressing strand was made of seven cold-drawn bright wires and stress relieved. The strand, produced by the American Steel and Wire Division, United States Steel Corp., was delivered in two coils. After release of prestress, several pieces of strand of varying length were saved for relaxation and other tests.

Tensile tests were made on 90 coupons of wire and on 33 coupons of strand. Typical stress-strain diagrams are shown in Figure 17. The following mean ultimate strengths were found:

- Wire, both shipments, ... 257 ksi
- Strand, shipment A, ..... 265 ksi
- Strand, shipment B, ..... 275 ksi

The mean cross-sectional area of the wire was 0.0293 sq. in.; that of the strand, 0.0806 sq. in.

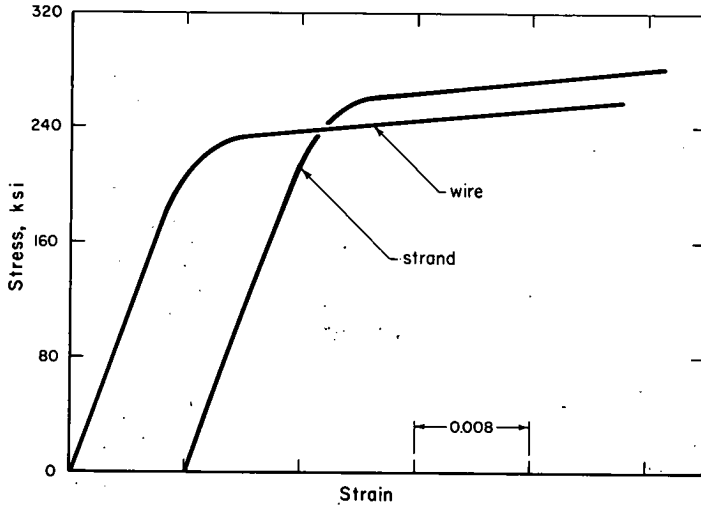


Figure 17. Typical stress-strain curves of prestressing steel.

The chemical composition of the steel was determined by analyses of three samples for each shipment. The averages are given in Table 7.

TABLE 7  
CHEMICAL COMPOSITION (%) OF WIRE AND STRAND

Element	Wire		Strand	
	Shipment A	Shipment B	Shipment A	Shipment B
Carbon	0.80	0.80	0.72	0.73
Manganese	0.67	0.63	0.71	0.78
Phosphorus	0.016	0.016	0.015	0.017
Sulfur	0.040	0.037	0.034	0.040
Silicon	0.25	0.25	0.23	0.24

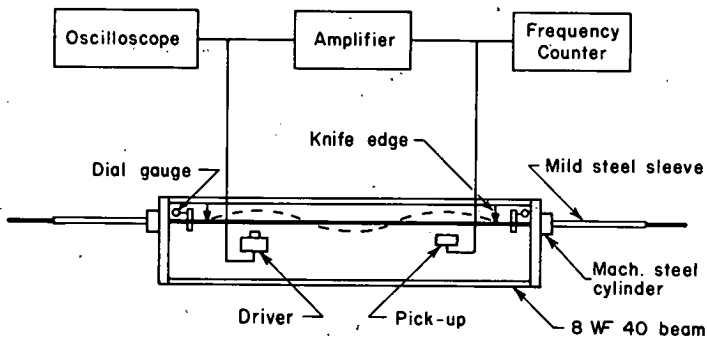


Figure 18. Testing apparatus for wire.

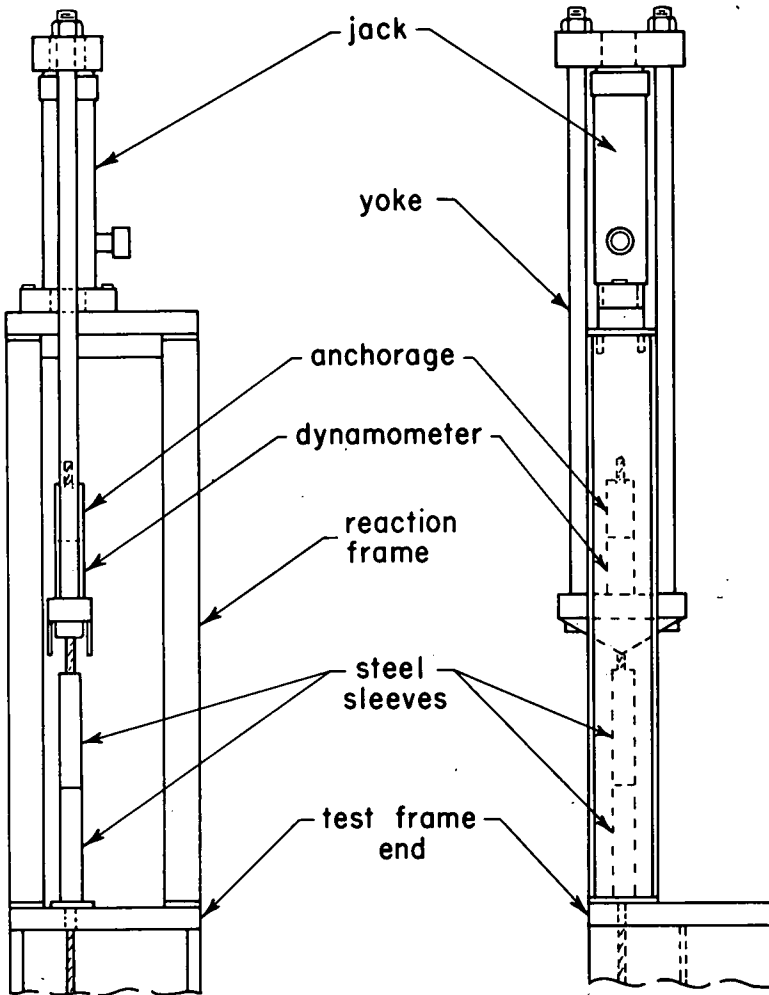


Figure 19. Jacking assembly for wire and strand.

### Testing Apparatus and Instrumentation

Wire and strand specimens were tested in frames, shown schematically in Figure 18. The frames were made from 36-in. lengths of 8WF40 beam with plates welded on each-end. The wire or strand was anchored with mild steel sleeves crimped on the specimen. For wire specimens the bearing area of the anchorage was increased with a steel cylinder into which the sleeve was press-fitted. The anchorage bore against steel shims which in turn bore against wedges.

The initial stress was applied with the jacking assembly shown in Figure 19. It consisted of a 10,000-psi hydraulic jack, a reaction frame, a yoke, a dynamometer, and a wedge-type grip anchorage.

The initial stress and the relaxation stress losses in strands were determined with a calibrated load cell placed in an assembly as shown in Figure 20. The cell was seated on a reaction frame bearing against the testing frame. A yoke transmitted the force from the strand to the load cell. The response of the load cell was monitored by a strain indicator with one division corresponding to 48 lb.

The initial stress in the wires was determined with a calibrated dynamometer made of an aluminum cylinder. The dynamometer was incorporated into the jacking assembly shown in Figure 19. The response of the dynamometer was monitored by a

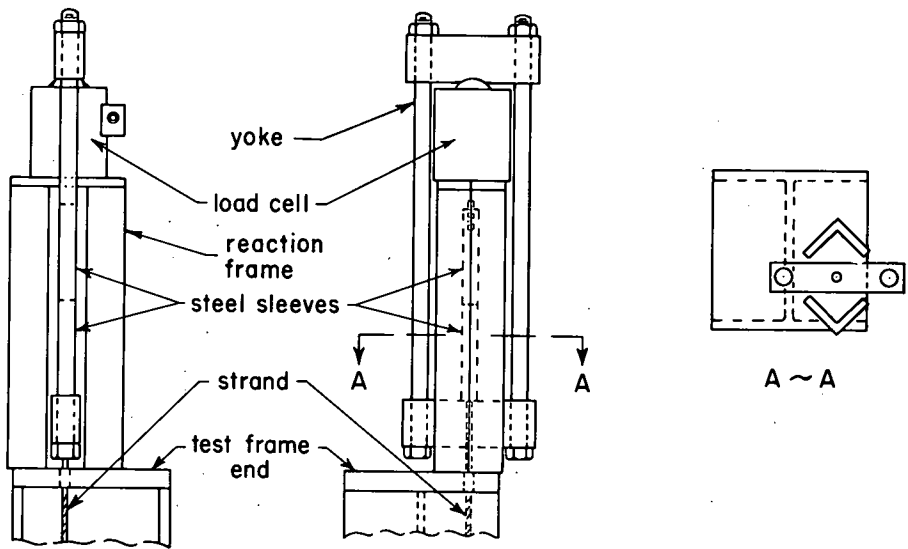


Figure 20. Load cell assembly for strand.

strain indicator with one division corresponding to 17 lb.

The relaxation stress losses in the wires were determined by measurements of the third mode of the fundamental frequency of lateral vibration of the wires. The fundamental frequency of lateral vibration of a wire depends essentially upon the tension in the wire and to a lesser degree upon the effect of the wire resting as a simply-supported beam (9). The relationship between the frequency and stress was obtained experimentally during initial loading of each specimen. Within the range of the test data, the stress was found to be a linear function of the frequency squared, but the calibration lines did not pass through the origin.

Measurements of the frequency required a pick-up, a five-digit frequency counter, an amplifier, a driver, and an oscilloscope, as shown schematically in Figure 18. The pick-up was of standard magnetic type used on musical instruments. The driver was built of a 500-ohm relay coil and a permanent magnet. A standard oscilloscope was inserted into the system to provide a check against excessive amplification of the wire vibration.

The wave length was determined by two knife edges supported from the test frame 28 in. apart. The driver and the pick-up were placed at the outer 1/6 points between the knife edges.

Slippage in the anchorages of both the wires and the strands was checked with two dial gages graduated to 0.0001 in. One gage was mounted near each end of the test frame and was resting on a collar attached to the specimen.

### Loading and Testing Procedures

For the tests of strand, the specimen was stressed with the hydraulic jack 20,000 psi in excess of the desired level, the overstress being required to compensate for losses caused by seating of anchorages. Steel wedges were then inserted between the anchorage sleeve and the loading frame and the jack was released. The strand was overstressed for no longer than one minute.

Load cell readings were taken before and immediately after loading, and were continued at intervals to measure the loss of stress in the strand. Readings were taken on the basis of a logarithmic interval with approximately 10 readings per cycle taken between 1 1/2 min to 100 hr, and from 15 to 20 readings between 100 to 1,000 hr. On two specimens readings were also taken approximately every 1,000 hr to over 9,000 hr. The readings were believed accurate to about 100 psi.

While the initial readings were taken, the collars for the dial gages were attached to the strand and zero readings on the dial gages were recorded. Before every subsequent reading of the load cell, the dial gages were checked. There were no indications of anchorage slippage on any specimen throughout the testing period.

In the tests of wire, the initial loading procedure had to include the determination of the stress-frequency relationship. The load was applied to the wire in increments and the frequency, as well as the dynamometer response, was noted for each increment. An overstress of 19,000 to 24,000 psi was required to seat the wire at the desired stress level. The overstress was held for 20 to 30 sec, the time required to position wedges between the anchorage and the frame. If the desired stress level was not reached upon the release of the jack, the specimen was overstressed a second time, and a third time if necessary. The entire loading procedure took 5 min at the most.

After the wire was secured in the frame, the initial frequency reading was taken as quickly as possible. Subsequent readings were taken at the same time intervals as those chosen for the strand. One hour after loading, the collars were put on the wire and initial readings on the dial gages were taken.

The procedure for determining the stress loss in the wire was somewhat more complicated than for strand. After checking the dial gages for any movement in the time interval between readings, the collars attached to the wire had to be taken off as they would change the mass of the vibrating wire and thus also the frequency-stress relationship. The wire was excited by plucking. The position of the driver and pick-up coils produced the third mode of the fundamental frequency. (The third mode was chosen for two reasons. First, the change of frequency encountered in the wire was least affected by other influences, such as unknown and conditions and vibrations of the frame or instruments. Second, the change in stress due to relaxation losses was such that the third mode gave a range of frequency sufficient in relation to the sensitivity of the measuring system.) By adjusting the amplifier, the amplitude of the wire vibration could be controlled and an undistorted wave seen on the oscilloscope. The frequency, measured with a frequency counter, was read over a 10-sec interval to obtain a reading of one-tenth of a cycle or approximately 40 psi. However, the overall accuracy depended also on the calibration of the dynamometer and was estimated to be within 100 psi.

As in the case of strand, no indications were found of any anchorage slippage in the wire tests.

## *Appendix C*

### ANALYSIS OF TEST RESULTS

The time-dependent losses were assumed to be described by the mathematical model given as Eq. 4, which in its linearized state (Eq. 4a or 4b) can be written as

$$\Sigma X_1 = A + bX_2 + \text{residual}$$

The least squares normal equations that will minimize the sum of squared residuals are:

$$\Sigma X_1 = N A + b \Sigma X_2 \tag{8a}$$

$$\Sigma X_1 X_2 = A \Sigma X_2 + b \Sigma X_2^2 \tag{8b}$$

in which component parts  $X_1$  and  $X_2$  constituted measured test variables and  $N$  was the number of test data used in the analysis. The coefficients  $A$  and  $b$  were determined by simultaneous solution of Eq. 8a and 8b. This method was used to fit all shrinkage data, and creep and relaxation data for individual tests.

For relaxation stress losses and creep strains, the potential time-dependent loss  $\Delta_{\infty}$  was expressed in terms of the initial load and ultimate strength (Eq. 6a and 7a).

The linearized equation that represents three variables has the form

$$X_1 = A + c X_2 + b X_3 + \text{residual}$$

Multiple regression analysis must now be used and the least squares normal equations that will minimize the sum of squared residuals for the linear series were

$$\Sigma X_1 = N A + c \Sigma X_2 + b \Sigma X_3 \quad (9a)$$

$$\Sigma X_1 X_2 = A \Sigma X_2^2 + b \Sigma X_2 X_3 \quad (9b)$$

$$\Sigma X_1 X_3 = A \Sigma X_3 + c \Sigma X_2 X_3 + b \Sigma X_3^2 \quad (9c)$$

in which the component parts  $X_1$ ,  $X_2$  and  $X_3$  constituted the measured variables. These equations were solved simultaneously for the values of coefficients  $A$ ,  $c$  and  $b$ .

The solutions of Eq. 8 and 9 were programed for the electronic computer used at the Road Test. Separate analyses were made for shrinkage, creep and relaxation with the component parts of the equations expressed as outlined in the following.

### Shrinkage Analysis

The shrinkage data showed a well-defined seasonal variation, which appeared to be superimposed on a long-time trend. The method of moving averages was used to extract this long-time trend from the test data. The moving averages were established in the following manner:

1. The test period was divided into 25 monthly intervals.
2. It was observed that the seasonal effect was approximately one year in length; therefore, the data for the first twelve intervals was averaged, giving an average at the sixth period.
3. Next the data for the first 13 intervals minus the first interval was averaged giving the moving average at the seventh period. This was continued until the nineteenth period, giving a total of fourteen moving average points.

The moving averages for the four specimens were averaged ( $\bar{\Delta}_s$ ) and then fitted with Eq. 4a. As shrinkage is not a function of load and all concrete was of the same quality, the total potential shrinkage contained no independent variable. Therefore, Eq. 8a and 8b were used to obtain the regression coefficients. The component parts were

$$X_1 = \log(\bar{\Delta}_s + Z) = \log \Delta'_s$$

$$X_2 = \log(1 - e^{-t/a})$$

and

$$A = \log \Delta_\infty$$

in which  $Z$  represents an estimate of shrinkage strain that occurred before the measurements were started. It was assumed in the analysis that  $Z$  corresponded to the shrinkage strain at  $t = 18$  days.

The analysis was repeated for several chosen combinations of  $a$  and  $Z$  values. The best correlation corresponded to the following values of coefficients:  $Z = 0.0001$ ;  $a = 166$ ,  $\Delta_\infty = 0.00028$ , and  $b = 0.50$ .

The differences between the shrinkage data, corrected by the term  $Z = 0.0001$ , and the strains computed from Eq. 5a were evaluated next. These residuals ( $\Delta''_s$ ) showed a seasonal variation following the trend of a sine wave. Attempts were made to correlate the residuals to the relative humidity. Although some correlation was found with the monthly average relative humidity in Peoria (Fig. 16), better results were obtained by correlation with the time of the year utilizing the equation of a sine wave having length equal to 364 days. Therefore, the equation of a sine wave was selected for the mathematical model. The sine term was modified by function  $(1 - e^{-t/X})$  to

satisfy the boundary condition at time  $t = 0$ .

The resulting model used for the regression analysis of the residuals was

$$\Delta''_s = A + b(1 - e^{-t/x}) \sin \frac{\pi(t' + \phi)}{182} \tag{10}$$

so that the component parts of Eq. 8a and 8b were

$$X_1 = \Delta''_s$$

$$X_2 = (1 - e^{-t/x}) \sin \frac{\pi(t' + \phi)}{182}$$

The constant 182 was selected on the basis of a one-year cycle. The constant  $x$  was selected so that the cyclic variation would have little influence on shrinkage before six days of age and full influence after thirty days. A value of  $x = 10$  appeared to fulfill this condition. Analyses were then made with several chosen values of the phase angle  $\phi$  and the following constants were found to give the best correlation:  $x = 10$ ,  $\phi = 60$ ,  $A = 0.000000$ , and  $b = 0.000087$ .

Creep Analysis

The creep data were analyzed in two steps. The first entailed fitting Eq. 4a to the data of individual creep tests. The component parts of Eq. 8a and 8b were

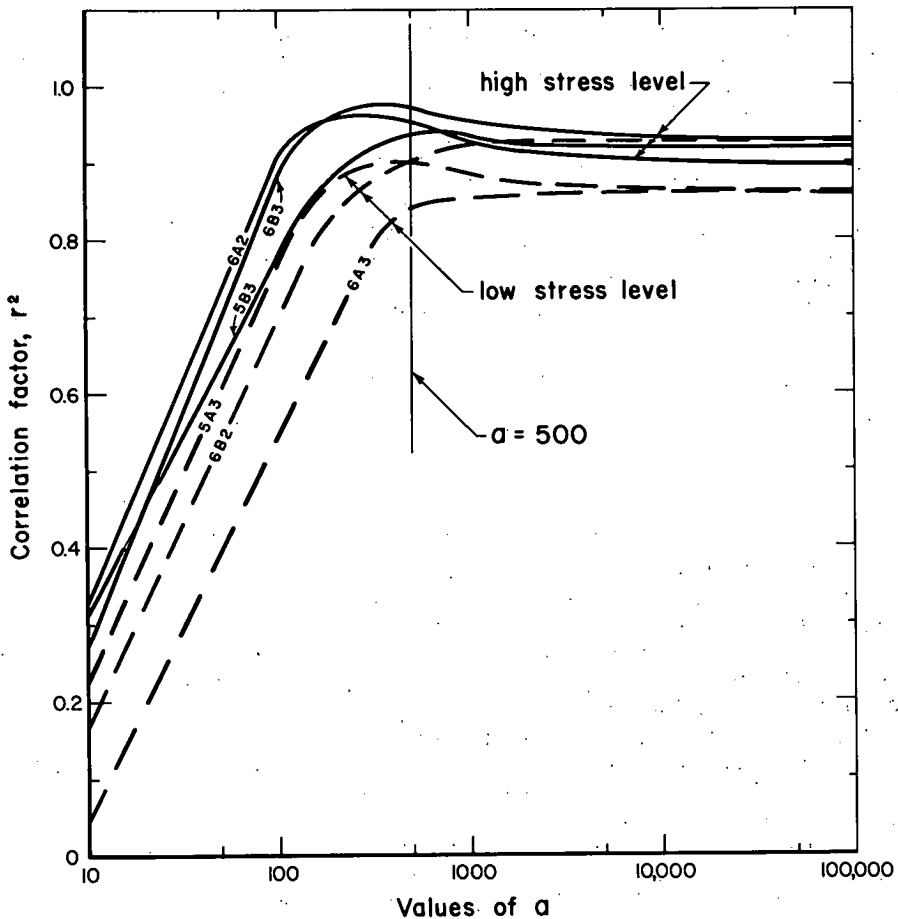


Figure 21. Variation in correlation with choice of a.

$$X_1 = \log \Delta_c$$

$$X_2 = \log (1 - e^{-t/a})$$

The results of fitting the individual creep tests assuming different values of  $a$  are shown in Figures 21 and 22. Figure 21 shows the variation in the correlation coefficient for different values of  $a$ . Figure 22 shows the change in total potential creep for each specimen as the coefficient  $a$  is changed. From studies of the test data and Figures 21 and 22, a choice of  $a = 500$  appeared to give reasonable values of  $\Delta_{\infty}$  corresponding to high correlation coefficients for each specimen.

Analyses using  $a = 500$  are reported in Table 8. No large variation in coefficient  $b$  was noted.

The final step in analyzing the creep data was a combined regression analysis of tests 5A3, 5B3, 6A2, 6A3, 6B2 and 6B3, using the constant  $a = 500$ .

A combination of Eq. 4 and 6a, used for this purpose, resulted in the transformed form:

$$\log \Delta_c = \log A + c \log \frac{f_{ci}}{f_{ci}} + b \log (1 - e^{-t/a}) \quad (11)$$

Eq. 9a, 9b and 9c were used to obtain the regression coefficients. The component parts were

$$X_1 = \log \Delta_c$$

$$X_2 = \log \frac{f_{ci}}{f_{ci}}$$

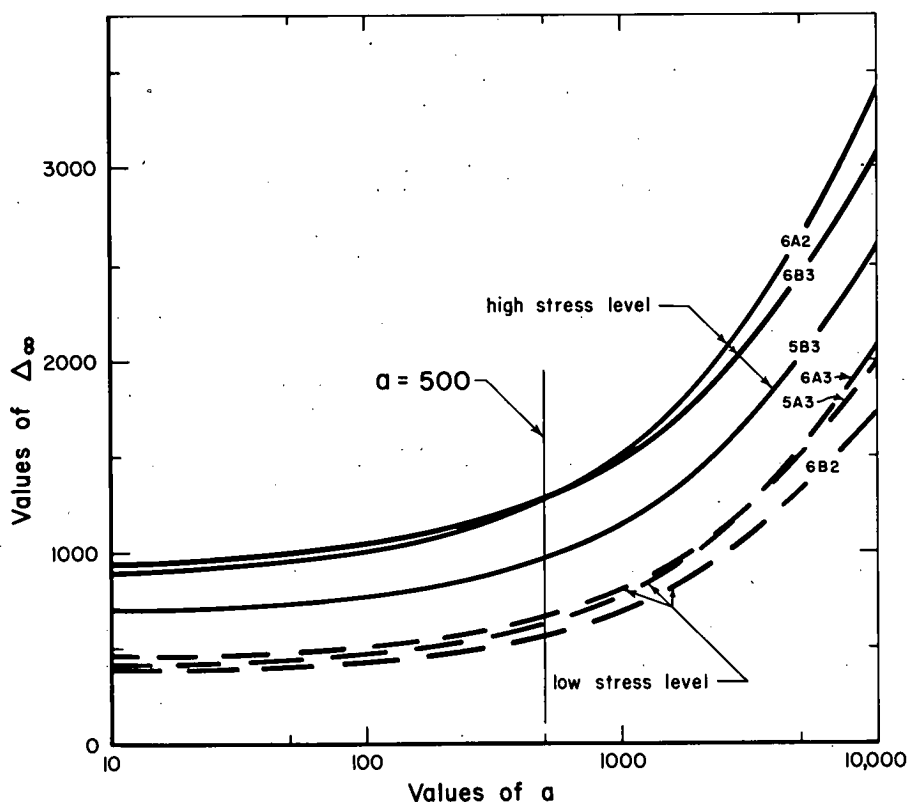


Figure 22. Variation of  $\Delta_{\infty}$  with choice of  $a$ .

$$X_3 = \log (1 - e^{-t/500})$$

The combined regression analysis gave the coefficients:  $A = 0.00356$ ,  $c = 0.96$ , and  $b = 0.73$ .

The value of  $c = 0.96$  shows that the effect of  $f_{ci}/f'_{ci}$  was practically linear.

TABLE 8  
REGRESSION COEFFICIENTS FOR INDIVIDUAL CREEP  
TESTS WHEN  $a = 500$

Load = 1,000 psi				Load = 2,000 psi			
Test	$\Delta_{\infty 1}$	b	$r^{2*}$	Test	$\Delta_{\infty 1}$	b	$r^{2*}$
5A3	666	0.77	0.90	5B3	972	0.67	0.93
6A3	625	0.82	0.83	6A2	1261	0.72	0.95
6B2	574	0.75	0.91	6B3	1256	0.63	0.97

\*r = coefficient of correlation.

### Relaxation Analysis

The relaxation data also were analyzed in two steps. Each individual test was first fitted with Eq. 4b. The component parts of the equation were:

$$X_1 = \log \Delta_r$$

$$X_2 = \log t$$

The coefficients of regression for each individual specimen of wire and strand are given in Table 9. Coefficients b were reasonably uniform but the value of A decreased

TABLE 9  
REGRESSION COEFFICIENTS FOR INDIVIDUAL WIRE AND STRAND TESTS

Specimen	Initial Stress, $f_i$ , (ksi)	A	b	$r^{2*}$	Specimen	Initial Stress, $f_i$ , (ksi)	A	b	$r^{2*}$
(a) 3/8-In. Strand									
604	187.5	1.970	0.240	0.993	606	195.5	1.810	0.274	0.996
609	185.0	2.050	0.251	0.985	608	189.0	1.535	0.238	0.978
610	165.4	0.830	0.243	0.945	603	185.8	0.445	0.409	0.991
607	163.0	0.727	0.259	0.948	601	169.3	0.609	0.303	0.967
602	158.0	0.469	0.304	0.870	605	168.3	0.935	0.262	0.971
(b) 0.192-In. Wire									
502	199.1	0.0205	0.192	0.989	507	196.4	0.0083	0.321	0.991
510	187.7	0.0043	0.338	0.997	505	184.7	0.0080	0.281	0.982
509	180.7	0.0235	0.199	0.996	504	181.0	0.0062	0.286	0.993
506	169.1	0.0150	0.231	0.994	503	175.0	0.0077	0.246	0.994

\*r = coefficient of correlation.

with a decrease in initial stress level. Furthermore, the order of magnitude of A was different for the strand, for wire from shipment A, and for wire from shipment B.

Studies have shown that the differences in the order of magnitude of coefficient A could not be explained in terms of the known differences in the properties of the strand and wire. Therefore, three separate multiple regression analyses of the combined data were performed, one including all strand specimens, one including all wire A specimens and one including all wire B specimens.

Eq. 7 was the basic equation for the multiple regression analyses of relaxation data. In linearized form, it was

$$\log \frac{\Delta r}{f_i} = \log g + d \log \frac{f_i}{f_s} + b \log t \quad (12)$$

so that the component parts of Eq. 9a, 9b and 9c were

$$X_1 = \log \frac{\Delta r}{f_i}$$

$$X_2 = \log \frac{f_i}{f_s}$$

$$X_3 = \log t$$

The solution of Eq. 9a, 9b and 9c gave one set of coefficients g, d and b for each of the three multiple regression analyses. The coefficients are listed in the preceding text under "Relaxation Equations."